

Ignition Transition in Turbulent Premixed Combustion at Elevated Pressure

C. C. Liu, S. S. Shy*, M. W. Peng, H. J. Chung, Y. W. Hsiu

Department of Mechanical Engineering, Center for Energy Research, College of Engineering
National Central University, Zhongli City, Taoyuan County 32001, TAIWAN

1 Abstract

Just recently, Shy and his coworkers conducted a series of turbulent premixed combustion experiments at atmospheric pressure condition to measure the minimum ignition energy (MIE), a probabilistic variable of 50% ignitability, of methane-air mixtures over a wide range of the equivalence ratio ϕ varying from 0.6 to 1.3. They found a turbulent MIE transition, across which both values of MIE and ignition flame kernels change drastically. From their complete turbulent MIE dataset, a physical model based on a reaction zone Péclet number (P_{RZ}) defined as the ratio of turbulent to molecular diffusivities was then proposed to explain such turbulent MIE transition. Using the same ignition methodology, this work presents a complete data set of lean CH₄-air mixtures at $\phi = 0.7$ and an initial pressure $p = 0.3$ MPa under both quiescent and turbulent conditions, in which the normalized turbulent intensity u'/S_L are varied from 0 to about 80, where S_L is the laminar burning velocity. These high-pressure turbulent ignition experiments are conducted in a recently-established high-pressure double-chamber explosion facility, in which an inner chamber, similar to the previous fan-stirred cruciform burner used in the atmospheric condition, is resided in a very large high-pressure absorbing vessel (the outer chamber). It is found that values of MIE required for the same flammable mixtures at $p = 0.3$ MPa are lower than those measured at atmospheric pressure under either laminar or turbulent conditions. More importantly, a MIE transition is also found to exist in the present high-pressure turbulent ignition case, showing two different regimes. In the first regime, values of MIE are found to increase modestly with increasing u'/S_L up to 60. When values of u'/S_L are increased further, a very steep increase of MIE values can be found in the second regime right after the transition. Comparison of the present high-pressure MIE data with the previous atmospheric MIE data is presented in terms of P_{RZ} . It is shown that the critical value of P_{RZ} at which the MIE transition occurs is larger for the present high-pressure MIE measurement ($P_{RZ} \approx 6.3$) than that for the previous atmospheric case ($P_{RZ} \approx 4.5$). This implies that the threshold of turbulence level relative to chemical reaction for the mode transition from flamelet-like turbulent wrinkled kernel to distributed-like broken kernels needs raising in order to enhance turbulence at elevated pressure due to the need of smaller intense Kolmogorov eddies that are capable to break the high-pressure flame kernels with comparable size.

2 Introduction

Minimum ignition energy (MIE) is essential for understanding of the ignition process of explosive mixtures, is extremely important for safety standards, and is necessary for optimization of ignition systems [1]. MIE is a probabilistic variable indicating an ignition energy (E_{ig}) of 50% successful ignitability for a given combustible mixture, that is, $MIE \equiv E_{ig(50\%)}$, which can only be determined statistically by repeating the same ignition experiments. Recently, Shy and co-workers [2-4] conducted a series of turbulent ignition experiments in a fan-stirred cruciform burner at atmospheric pressure and obtained a complete MIE dataset of CH₄-air mixtures at six different values of the equivalence ratio ϕ ($= 0.6, 0.7, 0.8, 1.0, 1.2, 1.3$), each covering a wide range of the normalized turbulent intensity u'/S_L , where S_L is the laminar burning velocity. They found a turbulent MIE transition, across which both values of MIE and ignition flame kernels change drastically. Based on their complete MIE dataset, a reaction zone Péclet number ($P_{RZ} \equiv \nu_K \lambda / \alpha_{RZ} = u' \eta_K / S_L \delta_{RZ}$) defined as the ratio of turbulent to molecular diffusivities was proposed to explain the turbulent MIE transition and to construct a predictive model for turbulent MIE, where ν_K and η_K are the Kolmogorov scales respectively for velocity and length, λ is the Taylor length scale, and u' is the r.m.s. turbulent fluctuating velocity. Note that the reaction zone thermal diffusivity, $\alpha_{RZ} \approx S_L \delta_{RZ}$, is determined at the mean temperature between products and reactants, where δ_{RZ} is the laminar flame thickness and/or the ignition kernel (reaction zone) size. However, these previous MIE measurements at atmospheric pressure may probably be viewed as an approximation for most real turbulent combustion situations that occur in the high pressure environment such as internal combustion engines. Thus, there is a need to measure MIE data for both quiescent and turbulent conditions at elevated pressure.

Using the same ignition methodology as that previously used in [2-4], this work presents a complete data set of lean CH₄-air mixtures at $\phi = 0.7$ and an initial pressure $p = 0.3$ MPa under both quiescent and turbulent conditions, where values u'/S_L are varied from 0 to about 80. These high-pressure turbulent ignition experiments are conducted in a recently-established high-pressure, double-chamber, fan-stirred, large-scale explosion facility, as discussed below.

3 Experimental

Figure 1 shows the recently-built high pressure premixed turbulent combustion facility [5], where the high-pressure turbulent cruciform burner (inner burner) is depicted in dash lines and placed inside of the large high-pressure absorbing chamber (outer chamber). As the two fans of the inner burner driven by a pair of 10 HP motors which are counter-rotated at the same speed, a large volume up to $150 \times 150 \times 150$ mm³ of nearly homogeneous isotropic turbulence can be generated in the core region of the inner burner, having zero mean velocities and energy spectra with $-5/3$ decaying slope [6]. Moreover, the associated turbulent characteristics such as u' and the integral length scale (L_1) in this fan-stirred cruciform burner have been proven to be insensitive to pressure via PIV measurements [5], so that previous turbulent characteristics obtained by extensive LDV and PIV measurements at the atmospheric pressure condition [7] can be used even at the elevated pressure condition.

In order to safely handle the explosive gas expansion generated by intense turbulent combustion at elevated pressure, the inner burner is not only constructed using reinforced structures, but also equipped symmetrically with four sensitive pressure-releasing valves on its vertical vessel. Therefore, these pressure-releasing valves not only prevent danger of the explosive pressure rise inside the inner burner, but also provide an approximately constant pressure environment for both laminar and turbulent flame propagation during pressure releasing. Also plotted in Fig. 1 are schematics of other complementary systems including the spark electrode with the current monitor and the voltage probe as well as the oscilloscope, a high-voltage pulse generator with an adjustable ignition energy varying from 0 to about 200 mJ, an air compressor equipped with contaminant-removing filters and a dehumidifier, the combustible mixture supply system, the vacuum pump and gas exhaust system, the water cooling system, a separate high-pressure fan-stirred mixing chamber, and the high-speed high-

resolution image acquisition system using a Vision Research Phantom v310 COMS camera. The gap-adjustable spark-electrode is positioned at the central region of the inner chamber. For simplicity, we keep the electrode gap constant for all experiments conducted here at 2.6 mm.

In this study, lean CH₄/air premixtures at $\phi = 0.7$ are used. The discharging energy released into the electrode gap can be adjusted from less than 0.1 mJ to higher than 100 mJ with a fixed spark duration time equal to 100 μ s. The realization steps of the high-pressure explosion experiment are as follows. In the beginning, both the inner burner and the outer chamber are purged by dry clean air and then the inner burner is deeply evacuated. During the process of gradually filling the combustible gas mixtures into the inner burner to the wanted pressure condition, the outer chamber is simultaneously pressurized by air at a pressure value at least equivalent to or slightly greater than the pressure inside the inner burner. Such procedure can prevent the combustible gas from leaking into the outer chamber via the sensitive pressure-releasing valves. A run then begins by centrally igniting the quiescent or random-flowing combustible mixtures at $p = 0.3$ MPa. Both current and voltage waveforms are recorded in an oscilloscope and thus the value of E_{ig} can be obtained by integration of the product of voltage and current throughout the spark duration. For confirmation of the successful ignition, the high speed camera is also used to simultaneously acquire the images of flame kernel formation and development into propagating flames.

Statistical values of minimum ignition energies obtain in the present study are measured according to the identical procedure used previously in Refs. [2-4]. Here we briefly review such procedure as follows. The first step is to determine the ignition energies with 0% and 100% ignitability ($E_{ig,0\%}$ and $E_{ig,100\%}$). A simple way to find $E_{ig,0\%}$ is to continuously discharge for at least 5 times while slowly increasing the ignition energy until the hardly ignited case occurs. For $E_{ig,100\%}$, a similar yet reverse way should be carried out to locate the rarely misfired case. When the $E_{ig,0\%}$ and $E_{ig,100\%}$ are approximately identified, three more E_{ig} points need measuring, and among these three points, the ignitability at the midpoint between $E_{ig,0\%}$ and $E_{ig,100\%}$ is the first to be measured. At least 10 identical runs were carried out to determine the ignitability. The measured ignitability of this first midpoint is then used to decide which direction the following two measurements should be taken. For example, if the ignitability of this midpoint is larger than 50%, then the next midpoint is selected just between the former midpoint and the $E_{ig,0\%}$. Likewise, the location and ignitability of the third midpoint can be determined. With these measured ignitabilities at three midpoints together with $E_{ig,0\%}$ and $E_{ig,100\%}$, the $E_{ig,50\%}$ can be interpolated by a spline-fit line.

4 Results and Discussion

Figure 2 shows the values of present high-pressure MIE as a function of the fan frequency (f). Also shown in Fig. 2 are the previous atmospheric MIE data. Here $u' = 4.62f$. It is found that values of MIE required for the same quiescent or flowing mixture at $p = 0.3$ MPa is lower than those at $p = 0.1$ MPa. Based on the concept that MIE should be at least capable to heat up a flame kernel of volume δ to its associated adiabatic flame temperature which is totally insensitive to pressure, the decrease of MIE with increasing pressure may be explained by the decrease of the flame kernel volume (δ) at elevated pressure. It is known that the laminar flame thickness (δ_f) decreases with increasing pressure and $MIE \sim \rho\delta \sim \rho\delta_{fz}^3 \sim \rho\delta_f^3$. Since $\delta_f \sim p^{-0.5}$ for methane flame, MIE is thus expected to decrease with increasing pressure even if the gas density $\rho \sim p$. Furthermore, the turbulent MIE transition is also found to exist at $p = 0.3$ MPa. However, the occurrence of turbulent MIE transition is shifted towards higher fan frequency at elevated pressure. For example, as pressure varies from $p = 0.1$ MPa to $p = 0.3$ MPa, the fan frequency at which MIE transition occurs varies from $f = 94$ Hz to $f = 128$ Hz. The MIE transition separates the variations of MIE with f or (u') into two different regimes. The first regime in which values of MIE are found to increase slightly with increasing u' extends from a very small value of u' to that just before the transition. However, a steep increase of MIE values with further increasing u' can be found in the second regime right after the transition. Figure 3 further shows the values of high-pressure MIE as a function of u'/S_L . Similar conclusions can also be found in this kind of plot.

Note that the linear-fit line segments in Fig. 2 and 3 are obtained independently according to the shown data points in each plot. Thus there is a small difference locations of Figure 4 finally shows the normalized values of high-pressure MIE (MIE_T/MIE_L) as a function of P_{RZ} , where MIE_T and MIE_L respectively represent the values of turbulent and laminar MIE. Also shown in Fig. 4 are the previous atmospheric MIE data and the associated predictive model based on P_{RZ} . We found in Fig. 4 that P_{RZ} can better explain why the turbulent MIE transition shifts to higher turbulence level at elevated pressure. Because the decreasing size of the flame kernel with increasing pressure leads to less disturbances and penetration by small turbulent eddies. This implies that the smaller flame kernel with increasing pressure becomes harder and harder to be broken. Therefore, the threshold of turbulence level relative to the molecular transport (or chemical reaction) for the mode transition from flamelet-like turbulent wrinkled kernel to distributed-like broken kernels needs to be raised at elevated pressure in order to generate more intense turbulence which comprises intense Kolmogorov eddies with much smaller size comparable to the high-pressure flame kernel. It is also surprising to find that the atmospheric ignition model with critical $P_{RZ} = 4.5$ for turbulent MIE prediction seems applicable to the present high-pressure data in spite of the different critical value of P_{RZ} (≈ 6.3) at which turbulent MIE transition occurs. However, more high-pressure experiments need carried out in the near future for further validation.

References

- [1] Lewis B, von Elbe G. (1987). Combustion, flame and explosions of gases. Academic Press Inc. (ISBN 0-12-446751-2).
- [2] Shy SS, Liu CC, Shih WT. (2010). Ignition transition in turbulent premixed combustion. Combust. Flame 157: 341.
- [3] Shy SS, Shih WT, Liu CC. (2008). More on minimum ignition energy transition for lean premixed turbulent methane combustion in flamelet and distributed regimes. Combust. Sci. Tech. 180: 1735.
- [4] Huang CC et al. (2007). A transition on minimum ignition energy for lean turbulent methane combustion in flamelet and distributed regimes. Proc. Combust. Inst. 31: 1401.
- [5] Liu CC et al. (2011). On interaction of centrally-ignited, outwardly-propagating premixed flames with fully-developed isotropic turbulence at elevated pressure. Proc. Combust. Inst. 33: 1293.
- [6] Shy SS, I WK, Lin ML. (2000). A new cruciform burner and its turbulence measurements for premixed turbulent combustion study. Exp. Therm. Fluid Sci. 20: 105.
- [7] Yang TS, Shy, SS (2005). Two-way interaction between solid particles and air turbulence: Particle settling rate and turbulence modification measurements. J. Fluid Mech. 526: 171.

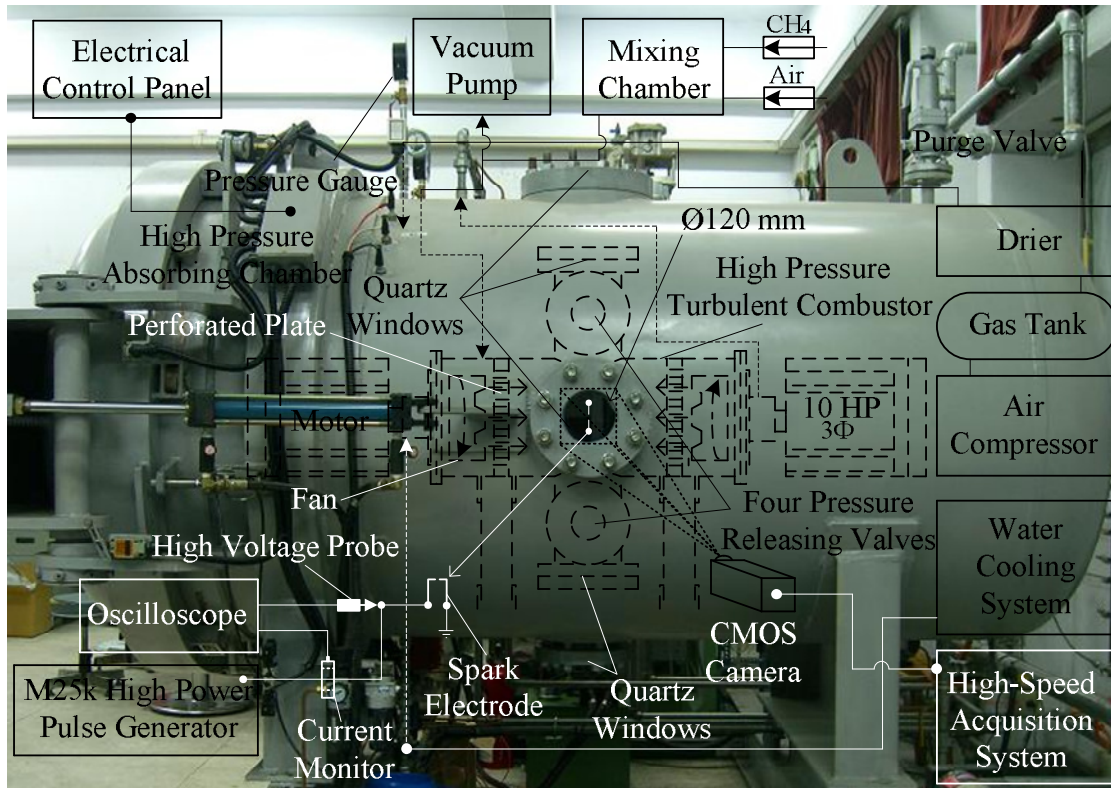


Figure 1. High pressure premixed combustion facility, including the high-pressure turbulent cruciform burner (inner burner) and the high-pressure absorbing chamber (outer chamber).

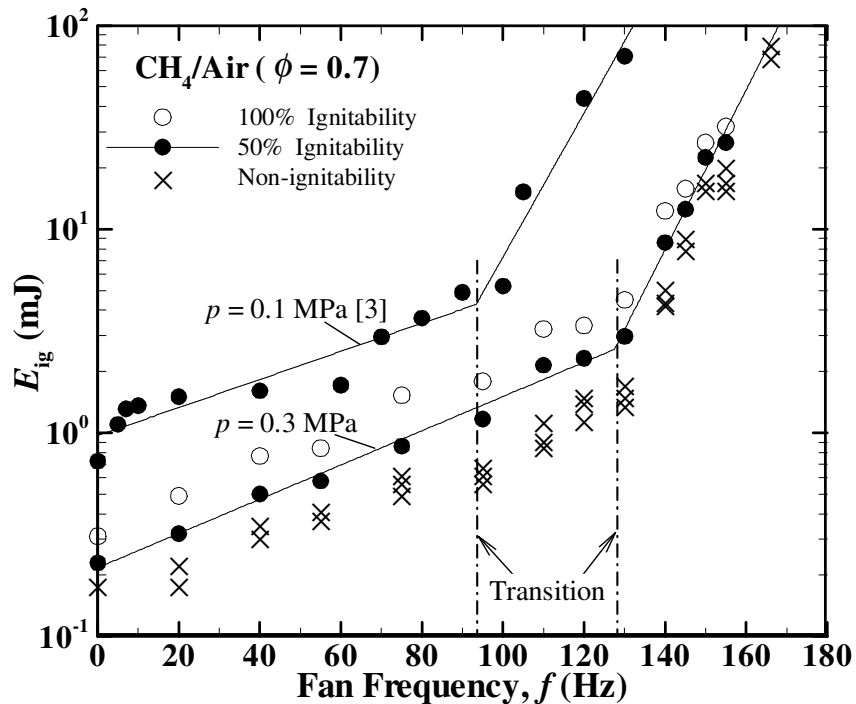


Figure 2. Variation of turbulent minimum ignition energy with the fan frequency.

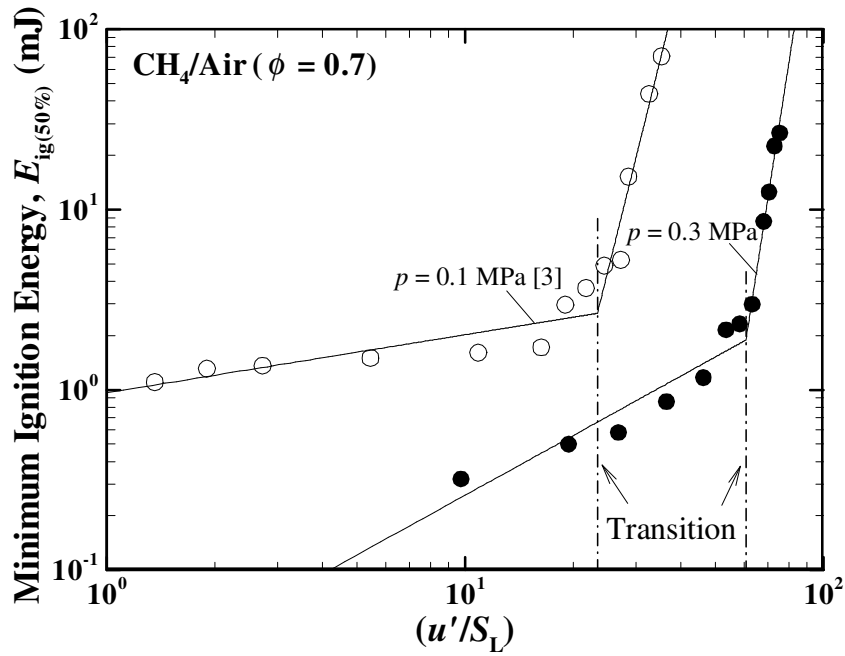


Figure 3. Variation of turbulent minimum ignition energy with normalized turbulent intensity.

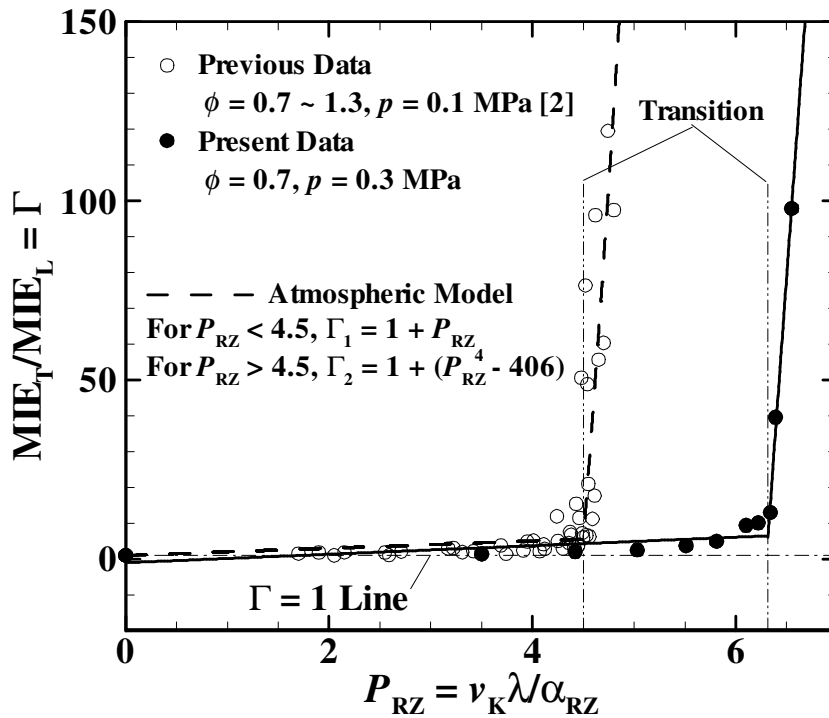


Figure 4. Variation of normalized minimum ignition energy with the reaction zone Péclet number.